YIV-906 Potentiated anti-PD1 Action Against Hepatocellular Carcinoma by Enhancing Adaptive and Innate Immunity in the Tumor Microenvironment.

Xiaochen Yang
China Academy of Chinese Medical Sciences
wing lam
Yale University School of Medicine
Zaoli Jiang
Yale University School of Medicine
Fulan Guan
Yale University School of Medicine
Xue Han
Yale University School of Medicine
Rong Hu
Yale University School of Medicine
Wei Cai
Yale University School of Medicine
William Cheng
Yiviva, inc.
Shwu-Huey Liu
Yiviva, inc.
Peikwen Cheng
Yiviva, inc.
Yuping Cai
Yale University School of Public Health
Nicholas J.W. Rattray
Yale University School of Public Health
Caroline H. Johnson
Yale University School of Public Health
Lieping Chen
Yale University School of Medicine
Yung-Chi Cheng (yccheng@yale.edu)
Yale University School of Medicine

Research Article

Keywords: YIV-906, immune enhancer, immunomodulator, PD1, PDL1, antiPD1, IDO, M1-like macrophages, tumor microenvironment

Posted Date: March 17th, 2021

DOI: https://doi.org/10.21203/rs.3.rs-289552/v1

Abstract

YIV-906 (PHY906) is a standardized botanical cancer drug candidate developed with a systems biology approach - inspired by a traditional Chinese herbal formulation, historically used to treat gastrointestinal symptoms including diarrhea, nausea and vomiting. In combination with chemotherapy and/or radiation therapy, preclinical and clinical results suggest that YIV-906 has the potential to prolong survival and improve quality of life for cancer patients. Here, we demonstrated that YIV-906 plus anti-PD1 could eradicate all Hepa 1–6 tumors in all tumor bearing mice. YIV-906 was found to have multiple mechanisms of action to enhance adaptive and innate immunity. In combination, YIV-906 reduced PD1 or counteracted PDL1 induction caused by anti-PD1 which led to higher T-cell activation gene expression of the tumor. In addition, YIV-906 could reduce immune tolerance by modulating IDO activity and reducing monocytic MDSC of the tumor. The combination of anti-PD1 and YIV-906 generated acute inflammation in the tumor microenvironment with more M1-like macrophages. YIV-906 could potentiate the action of IFNg to increase M1-like macrophage polarization while inhibiting IL4 action to decrease M2 macrophage polarization. Flavonoids from YIV-906 were responsible for modulating IDO activity and potentiating IFNg action in M1-like macrophage polarization. In conclusion, YIV-906 could act as an immunomodulator and enhance the innate and adaptive immune response and potentiate anti-tumor activity for immunotherapies to treat cancer.

Introduction

Hepatocellular carcinoma (HCC) is the most prevalent and aggressive type of liver cancer [1]. The median prognosis of patients with unresectable and recurrent HCC is only 3 to 7 months [2]. Sorafenib and Lenvatinib, which are multi-kinase inhibitors, were approved by the FDA as the first-line drug for HCC treatment [3]. Sorafenib and Lenvatinib have progression-free survival times of about 3.7 months and 7.4 months with serious adverse effects [4]. In 2017, the FDA granted Nivolumab (anti-PD1) accelerated approval to treat hepatocellular carcinoma (HCC) patients who do not respond to sorafenib. The objective response rate of Nivolumab was 20% and the percentage of patients with a complete response was only 1%, which is a significantly lower rate than for melanoma patients treated with Nivolumab [5]. Additionally, 32% of HCC patients did not even respond to Nivolumab. The therapeutic index for HCC patients treated with Nivolumab can be further improved.

YIV-906 is a standardized four-herb formulation based on an 1800-year old Chinese herbal formulation called “Huang Qin Tang”, which is prescribed to treat numerous gastrointestinal (GI) symptoms, including diarrhea, nausea, and vomiting. The highly refined concoction is composed of four herbs: *Glycyrrhiza uralensis* Fisch (**G**), *Paeonia lactiflora* Pall (**P**), *Scutellaria baicalensis* Georgi (**S**), and *Ziziphus jujuba* Mill (**Z**). Over a period of 18 years, six batch-to-batch consistent preparations of YIV-906 have been manufactured using cGMP standards and validated using quality control platforms including phytomics [6] and a recently developed mechanism-based quality control platform (Mech QC) to measure bioequivalence [7].

In seven Phase I/II to II clinical studies in liver, pancreatic and colorectal cancer at research institutions, including Yale University, Stanford University, UPMC Hillman Cancer Center and City of Hope Comprehensive Cancer Center, results from over 170 patients receiving irinotecan, capecitabine or chemo-radiation [8-11] in combination with YIV-906, reported no YIV-906-related toxicity at the dosage used along with zero-to-minimal Grade 3/4 non-hematological toxicities, including diarrhea, nausea, vomiting, fatigue - demonstrating improved quality of life as well as survival for patients.

In preclinical studies, YIV-906 was shown to enhance the anti-tumor activity of different classes of anti-cancer agents, including immune checkpoint inhibitors, tyrosine kinase inhibitors, topoisomerase inhibitors, anti-microtubule agents, alkylating agents, antimetabolites, and radiation in vivo [12]. YIV-906's mechanism of action for enhancing a broad spectrum of anti-cancer agents is primarily due to the induction of acute inflammation within the tumor microenvironment where infiltrated macrophages expressing more M1-like over M2-like phenotypes in the presence of a neo-antigen [13,14]. YIV-906 reduced irinotecan (CPT-11)-induced intestinal inflammation by inhibiting NFκB, COX-2, and iNOS while promoting intestinal stem/progenitor cell repopulation by simulating the Wnt signaling pathway [15]. In irradiation [16] studies, YIV-906 also reduced GI toxicity. YIV-906 could selectivity alternate the intestines' bacterial population; however, the microbe change is not responsible for YIV-906's action on irinotecan [17].

In this report, YIV-906 shows that it is an immunomodulator that can enhance the anti-tumor activity of anti-PD1 by promoting both adaptive and innate immunity through multiple mechanisms of actions via systems biology effect. Our results suggest YIV-906 may serve as a multitarget immune enhancer in the tumor microenvironment for immunotherapy for the treatment of HCC and other cancers.

Results

YIV-906 Enhanced Anti-PD1 Action to Inhibit Hepa1-6 Tumor Growth In Vivo and Demonstrated Tumor-Specific Vaccine-Like Effect

YIV-906 alone had no effect on Hepa1-6 tumor growth in vivo ($P > 0.05$) (**Fig. 1A and 1B**). Anti-PD1 alone started to slow down tumor growth of Hepa 1-6 on day 4 (**Fig1A and 1B**). Some tumors were shrunk on day 8 and 40% tumors were below detection limit at the end of the experiment (**Fig. 1A and 1B**).

Tumors responded to the YIV-906 plus anti-PD1 in as soon as 2 days with all tumors disappearing following 7-days of treatment ($P < 0.001$) (**Fig. 1A and 1B**). Without further treatment up to 21 days later, no tumors re-appeared in the YIV-906 plus anti-PD1 combination group. This suggested that the tumors had been "cured" in these mice (**Fig. 1A and 1B**). When Hepa 1-6 cells were re-implanted into the "cured" mice no tumor growth was found, while naïve mice had tumor growth (data not shown). When CMT167 cells (small cell lung carcinoma) or Pan02 (Pancreatic Ductal Adenocarcinoma) were implanted into the "cured" mice after being re-challenged with Hepa 1-6, CMT167 or Pan02 tumor growth could be observed. This behavior suggested YIV-906 in combination with anti-PD1 could create a tumor-specific vaccine-like effect.

In addition, YIV-906 could potentiate the action of anti-PD1 (70μg/animal and 200μg/animal) (**Fig S1).** It should be noted that the YIV-906 and anti-PD1 (70μg/animal) combination had a stronger anti-tumor effect than anti-PD1 200μg/kg (**Fig S1**). Therefore, YIV-906 could reduce the usage of anti-PD1 by at least 3-fold while achieving similar or better anti-tumor effects than anti-PD1 alone.

Combination of YIV-906 and Anti-PD1 Reduced Immune Suppression by Reducing the PD1 and PDL1 Protein Expression of Hepa 1-6 tumor

Since tumor shrinking happened on day 4 following YIV-906 plus anti-PD1, we compared apoptosis and DNA damage of tumors at this time point. YIV-906 plus anti-PD1 could significant increased levels of cleaved caspase 9 and DNA breakage (P-H2AX-ser139) **(Fig S2A, S2D and S2E)**. The above result supported that YIV-906 enhanced anti-PD1 action to lead to more cell death and tumor shrinkage.

The essential function of anti-PD1 is to restore cytotoxic T-cell function by inhibiting the co-inhibitory pathways of T cells through interrupting the interactions between PD1-PDL1[18]. As expected, anti-PD1 induced the number of activated T cells (GranyzmeB+/CD3+) of Hepa 1-6 tumors (**Fig 2A**). The number of activated T cell and Treg upon anti-PD1 treatment was not affected by the co-treatment of YIV-906 (**Fig 2B**). Interestingly, the combination treatment did induce more T cell activation related genes in Hepa 1-6 tumors (**Fig 2C**), suggesting that the function of T cells could be enhanced. We wondered if YIV-906 had an impact on PD1 and PDL1 protein expression leading to stronger T cell function. Results indicated that Anti-PD1 or YIV-906 alone did not change the PD1 tumor proteins (**Fig. 2D**). Compared to the control group or anti-PD1 alone group, YIV-906 plus anti-PD1 could significantly decrease PD1 tumor proteins (P = 0.02 or 0.003, respectively) following 4-day treatments (**Fig. 2D**). This result partially helps explain why less anti-PD1 combined with YIV-906 was required to have similar anti-tumor activity versus taking a higher dosage of anti-PD1 alone. Additionally, anti-PD1, but not YIV-906-only treatment, did significantly increase PDL-1 tumor protein (P =0.01) but this increase could be counteracted by combining YIV-906 and anti-PD1 (P=0.008) (**Fig. 2E**). These results suggested that YIV-906 might facilitate anti-PD1 action in overcoming tumor resistance to immune surveillance and lead to a stronger anti-tumor effect. Furthermore, anti-PD1 plus YIV-906 showed only moderate effects in slowing down the Hepa 1-6 tumor growth in nude mice (T cell deficient) (**Fig S3**). The synergistic effect between anti-PD1 and YIV-906 did require T cells involvement.

YIV-906 could modulated IDO activity and decreased MDSC of Tumor

IDO (Indoleamine 2,3-dioxygenase) is an enzyme responsible for metabolizing L-tryptophan into kynurenine. IDO expression could regulate T-cells (Tregs) [19] which help recruiting myeloid derived suppressor cells (MDSCs) into tumors to cause immune tolerance [20]. IDO could be a key resistance factor to anti-PD1 therapy[20,21]. We found that YIV-906 could modulate IDO activity in cell cultures (**Fig 3A**). After using purified *E.coli* glucuronidase (GU) to remove glucuronoside from chemicals to mimic the condition happening in lower GI, YIV-906GU had stronger IDO inhibition than YIV-906 (**Fig 3A**). Baicalein was shown to be the most potent compound among the flavonoids (**Fig 3A**). It was found that YIV-906 or YIV-

906/anti-PD1 had lower kynurenine/tryptophan ratio of Hepa 1-6 tumor (**Fig 3B**). This suggested that YIV-906 could modulate IDO activity in vivo. Furthermore, we found that anti-PD1 plus YIV-906 treatment reduced monocytic MDSC of Hepa 1-6 tumor (**Fig 3C**). Modulation of IDO by YIV-906 could be an additional mechanism action to reduce immune tolerance and facilitate the action of Anti-PD1.

YIV-906 plus Anti-PD1 Treatment Induced Macrophage Infiltration and Polarized to a Higher M1-like Macrophage Signature in Hepa 1-6 Tumors

The combination of YIV-906 plus anti-PD1, but not YIV906 alone or anti-PD1 alone, could significantly induce macrophage infiltration in Hepa 1-6 tumors after 4-days of treatment (**Fig. 4A and 4B**). This could be attributed to the increase of MCP1(CCL2), a monocyte chemoattractant protein, of tumors in the YIV-906 plus Anti-PD1 treatment group where MCP1 was higher than that of the anti-PD1 only group ($P<0.05$) (**Fig 4C and S4E)**). Depending on the tissue microenvironment, macrophages can be differentiated into two distinct phenotypes: M1 (tumor rejection) and M2 (tumor promotion). Based on bio-statistical analysis, YIV-906 plus anti-PD1 treatment had tumor environment favoring M1-like macrophages (**Fig. 4E and 4F**). Western blot analysis further confirmed that the iNOS protein (a M1 marker) but not Arg protein (a M2 marker) was substantially increased following YIV-906 plus anti-PD1 treatment (**Fig 4D and S5A-C**). This result also suggested that YIV-906 plus anti-PD1 treated tumors were highly inflamed. It is known that IFNg helps polarize macrophages into the M1-like state. We found that INFg mRNA expression of tumors was significantly induced by YIV-906 plus anti-PD1 treatment (**Fig 4E and S6C**). Therefore, the enhanced infiltration of M1-like macrophages induced by YIV-906 plus Anti-PD1, could be an additional mechanism aiding against Hepa1-6 tumor growth.

YIV-906 could Potentiate IFNg to Polarize Bone Marrow Derived Macrophages (BMDM) into M1-like Macrophage while Inhibiting IL4 to Polarize BMDM into M2-like Macrophage *in vitro*

As YIV-906 could promote more M1-like macrophage polarization, we investigated if YIV-906 had direct impact on polarizing BMDM into either M1-like or M2-like phenotype in culture. We first examined if β-glucuronidase treatment (GU), which could catalyze hydrolysis of β-D-glucuronic acid residues from certain chemicals could affect the macrophage polarization activity of YIV-906. The results indicated that YIV-906GU had a stronger induction effect on IFNg, IL1a, TFNa mRNA expression of BMDM than YIV-906 alone (**Fig 5A**). Furthermore, YIV-906 could potentiate IFN-γ to polarize BMDM into M1 macrophages with increased expression signals of iNOS, MCP-1, CXCL9, CXCL11, COXII, IL1a, TNF-α and CD86 (**Fig 5A**). GU treatment further enhanced the potentiation activity of YIV-906 on iNOS, IL1a, CXCL11(**Fig 5A**).

Conversely, YIV-906 could inhibit the action of IL4 for M2 macrophage polarization exhibited by the decreasing mRNA expression levels of Arg1, CD206 and IRF4 (**Fig** A). GU treatment could further increase the inhibitory activity of YIV-906 on Arg, IL10 and IRF4 mRNA expression in the presence of IL4 (**Fig 5A**).

We further studied if YIV-906 could affect the downstream events of the signaling cascade triggered by IFNg or IL4. In the presence of IFNg, YIV-906GU could further enhance P-Jak1/2 and P-Stat2

protein in as early as 30min. It could maintain higher P-Stat2 at 24h in the presence of IFNg in BMDM. At 24h YIV-906 or YIV-906GU potentiated IFNg in inducing iNOS protein expression but not the IFR1 protein of BMDM (**Fig 5B and S7A**). This could be because IFR1 might already have reached its maximum level at the given concentration of IFNg. In addition, IL15RA and ICAM mRNA could also be up-regulated by YIV-906GU in the presence of IFNg in BMDM (**Fig S8A and S8B**). YIV-906 or YIV-906GU potentiated IFNg action not limited to BMDM. but could also potentiate IFNg to induce MCP1, TNFa, iNOS mRNA in GM-CSF treated Raw cell 264.7 (macrophages) (**Fig S9**).

In contrast to IFNg, YIV-906 or YIV-906GU inhibited IL4 action by suppressing IRF4 expression, a key transcription factor of the IL4 signaling pathway (**Fig 5C and S7B**). Following 24h treatment of YIV-906 or YIV-906GU, inhibition of IL4 also led to down-regulation of Arg protein in BMDM (**Fig. 5C and S7B**). The decrease of IFR4 and Arg protein could be attributed to down-regulation of their mRNA by YIV-906 or YIV-906GU in the presence of IL4 (**Fig 5A**).

Our results demonstrated that YIV-906 or YIV-906GU could also potentiate IFNg action by stimulating P-Jak1/2 and P-Stat2 phosphorylation while inhibiting IL4 action by the IFR4 protein down-regulation of BMDM. The modality could explain how multiple mechanisms of YIV-906 can work to polarize macrophages into the M1-like phenotype. The immuno-modulatory effect of the above activities could be explained by the sugar moiety of chemicals present in YIV-906, specifically the aglycone chemicals which appear most active.

Flavonoids Play Key Roles of YIV-906 in Potentiating IFNg action to Polarize Macrophages into M1-like type

The key YIV-906GU components responsible for potentiating the IFNg action on macrophages were investigated. Of the four herb ingredients in YIV-906GU: **G**, **P**, **S** and **Z**, results indicated that **S**, in the presence of IFNg, had the highest biological activity on increasing iNOS/Arg ratio (**Fig. 6A**). Consistently the formulations without S (-S) completely lost the IFNg potentiation property (**Fig. 6A**). Key flavonoids (baicalein wogonin, chrysin, oroxylin A and baicalin) of **S**[22,23] could increase the IFNg action to increase iNOS/Arg ratio (**Fig. 6B**). Deleting any one herb of YIV-906 could reduce the potentiation of IFNg action (**Fig. 6A**). These results indicated that G, P, Z could also play a role in the IFNg potentiation or interact with S to enhance IFNg action.

Most importantly, the amount of wogonin and oroxylin A in the tumors was higher in the YIV-906 plus anti-PD1 group compared to the YIV-906 alone group (**Fig. 6C, Table S2**). Thus, these flavonoid compounds naturally present in component S in the YIV-906 plus Anti-PD1combo could be the active ingredients, along with others, contributing to the IFNg potentiation that polarizes macrophages to the M1-like phenotype in Hepa 1-6 tumors.

Discussion

Many current immune therapies for cancer are trying to convert "cold tumors" into "hot tumors" so that revived immune cells could attack tumor cells. Immune check point antibodies, such as anti-PD1, anti-PDL1, anti-CTLA4 have led to breakthroughs for the treatment of many tumor types; However, tumor types such as HCC, pancreatic and colon cancers have had relatively low response rates to these antibodies. Currently hundreds of remedies are being tested to see if they can further improve the efficacy of these immune check point antibodies. Many of these new remedies are designed to target a specific target (vs multiple targets) of the immune cycle. Up to date, there have been no major breakthroughs in these combination clinical trials. Here, we reported that YIV-906, a botanical immunomodulator with a systems biology effect, could potentiate anti-PD1 action against Hepa 1-6 tumor growth by promoting both adaptive and innate immunity through multiple mechanisms of actions.

For adaptive immunity, we found YIV-906 plus anti-PD1 could decrease PD1 tumor proteins and inhibited PDL-1 expression induced by anti-PD1. This could foster a more favorable tumor microenvironment for T cell activation. In addition, we found that YIV-906 could modulate IDO activity and leading to a decrease of MDSC of Hepa 1-6 tumor. We identified that flavonoids of **S** herb played a key role in modulating IDO activity. This result was supported by a previous report [24]. IDO inhibitors were reported to enhance the action of anti-PD1, anti-PD-L1, anti-CTLA4 on different types of animal tumors [20,21,25]. BMS-986205, with less side effects compared to Epacadostat which had serious adverse effects [26] and failed in clinical trials[27], is still being tested in combination with Nivolumab as first or second line therapy for liver cancer [NCT03695250].

In addition to adaptive immunity, YIV-906 also enhances the innate immune response. YIV-906 plus anti-PD1 could attract more M1-like macrophage infiltration which could be partly due to the induction of MCP1 in the tumors. Interestingly, YIV-906 also increased M1-like macrophage tumor infiltration when combined with irinotecan (CPT-11) or Sorafenib [13,14]. There is increasing evidence to support M1-like macrophages in tumors could enhance the efficacy of chemotherapy and target therapies [13,28,29]. It has also been reported that M1-like macrophages phenotype help T cells re-activation under immune checkpoint blockade therapy [30]. PD1 expression was found to dictate macrophage polarization. M2 macrophages, which have high PD1 expression and low phagocytic activity, promote tumor growth and are not favorable for immunotherapy [31]. In contrast, low PD1 expression favors M1-like macrophages that have high phagocytic activity and could increase immune check point blockade therapy action [31,32]. A recent report demonstrated that anti-PD1 could help switch macrophage polarity states from M2 to M1-like phenotypes in lung cancer [33]. Our result also indicated that anti-PD1 alone increased the probability of M1-like macrophage in the tumor microenvironment by 40%. Most importantly YIV-906 combined with anti-PD1 could further enhance M1-like macrophages and the innate immune response in the tumor microenvironment. YIV-906 plus anti-PD1 even further decreased PD1 proteins in tumor tissues which subsequently created favorable conditions for M1-like macrophage polarization [31]. The decrease in PD1 protein levels in the YIV-906 plus anti-PD1 group also explains why lower dosages (by 1/3), of anti-PD1 combined with YIV-could also achieve the same anti-tumor activity for higher doses of anti-PD1.

The combination not only eradicated the Hepa 1-6 tumors in every mouse, it also mimicked tumor-specific vaccine-like behavior as demonstrated by selective rejection of re-implanted Hepa 1-6 tumors and the growth of implanted CMT167 or Pan02 tumors. Some studies suggest that boosting innate immunity could increase tumor vaccine effect. A recent report demonstrated that exosomes secreted by M1-like macrophages can potentiate cancer vaccine-like properties through Th1 cytokine induction [34] resulting in a proinflammatory tumor climate. A separate study reporting that M1-like macrophages function by aiding CD8 T cell differentiation into memory T cells [35]. Our next step would be to investigate the extent exosomes or T-cells play in the vaccine mimicking behavior.

IFNg plays an important role in macrophage M1-like polarization. YIV-906 could potentiate the IFNg activity to turn up the signaling transduction response to a higher level; as anti-PD1 alone could activate T cells which released IFNg in tumor, adding YIV-906 could further amplify the IFNg signal and enhance M1-like macrophage polarization. Another unique property of YIV-906 was the inhibitory activity demonstrated on the M2 inducer, IL4, through down-regulation of IFR4. When treated with the combination of YIV-906 and anti-PD1, the dual effect of promoting M1-like polarity while inhibiting the M2 state ensures the dominance of M1-like macrophages in tumor tissues. Currently, there was no other therapeutic agents that can have these synergistic systems biology properties.

We identified *Scutellaria baicalensis Georgi* (S) as the key herb ingredient that is most likely responsible for promoting M1-like macrophage polarization. This result was consistent with our previous study of the effects of YIV-906 in combination therapy with anti-cancer drugs CPT-11 or sorafenib. Similar elevated predominantly M1-like macrophage signals were observed, as well as the enhanced anti-tumor activity of the combination [13,36]. Flavonoids were identified as the active compounds in S that promotes M1-like macrophage polarization. The flavonoid baicalin's ability to induce repolarization of tumor-associated macrophages to M1-like phenotype was demonstrated by others [37]. Most importantly, we detected baicalein, wogonin and oroxylin A in the Hepa 1-6 tumor and they could potentiate IFNg in the tumor to polarize macrophages into M1-like.

In conclusion, YIV-906 enhanced the anti-tumor activity of anti-PD1. The action is due to its ability to promote both adaptive and innate immunity. Flavonoids from *Scutellaria baicalensis Georgi* (S) were identified as one of the major active compounds responsible for modulating IDO activity, which regulated MDSC function and potentiated IFNg action to polarize macrophages into M1-like type. It could be interesting to investigate other herbs or herbal formulations containing S or flavonoids on anti-PD1 actions. YIV-906 component herbs G, P, Z might also contribute to the activity of YIV-906 and this is under current investigation. The potential use of YIV-906 as an immunomodulatory enhancer of tumor microenvironment in combination with Anti-PD1, or other immune check point antibodies, for the treatment of HCC or other type of cancers should be explored further in the clinic.

Material And Methods

Animal Studies

Details of animal studies can be found in our previous reports[13,15]. Briefly, Hepa 1-6 cells (about 2×10^6 cells in 100µl phosphate-buffered saline) were transplanted subcutaneously into 8-week-old female C57BL6 mice (Charles River Laboratories, Wilmington, MA). Body weight, tumor size, and mortality of the mice were monitored daily. After 10-14 days, mice with tumor sizes of 180 mm^3 were selected. Tumor volume was examined by using the formula length × $width^2$ × π/6. Each group consisted of seven mice. YIV-906 was administered orally for 7 days (500 mg/kg po, twice per day), while anti-PD1 was administered intraperitoneal on day zero (200ug/mice). In the control groups, mice were administered water orally. On Day 0, YIV-906 was administered 30 minutes prior to anti-PD1 administration. All animal experiments were carried out in accordance with the relevant guidelines and regulations approved Yale University Institutional Animal Care and Use Committee (IACUC) protocol. Animal experimental protocols were approved by Yale University Institutional Animal Care and Use Committee (IACUC). Animal studies were carried out in compliance with the ARRIVE guidelines.

Immunohistochemistry

After 4-day treatments, mice were terminated by cervical dislocation two days or four days after initiation of drug treatment (see above). Details of immunohistochemistry protocol can be found in our previous reports[13,15]. Intestinal and colon tissues were removed, fixed in formalin, embedded in paraffin, and sectioned into 10mm. The sections were mounted on Superfrost slides, dewaxed with xylene, and gradually hydrated. Antigen retrieval was achieved by 10mM Sodium citrate pH6.0 with 0.02% Tween-20 under steaming for 30 minutes. The source and dilution of primary antibody are listed in supplementary methods. The primary antibodies were diluted using Tris-HCl buffer containing 1% BSA and 0.5% Tween-20 and were incubated at room temperature for one hour. As a negative control, a set of slides was processed without primary antibody. Super-picture immunohistochemistry detection kit (Invitrogen, Inc.) was used for detection. The slides were counterstained with hematoxylin and mounted. The antibodies used were: Cleaved Caspase-3 (#9664, Cell Signaling Technology, Inc.), Cleaved Caspase-8 (#9496, Cell Signaling Technology, Inc. Danvers, MA), Cleaved Caspase-9 (#ab52298, Abcam, Cambridge, England), F4/80 (#ab16911, Abcam).

Flow cytometry analysis

Tumor tissues (200mg) were cut into small pieces in 0.5ml RPM1 640 culture medium. Liberase was added to dissociate the connected tumor cells at room temperature for 15 minutes. Dissociated cells were passed through a cell strainer (70um). After spinning down the cells at 1000g centrifugation for 10min, red blood cells were lysed with 1ml BD pharm lyse on ice. Cells were collected at 1000g centrifugation for 10min. $2x10^6$ cells were used for each staining sample. Cells were resuspended in RPM1 640 with 3% FBS. Anti-mouse CD16/CD32 clone 2.4G2 (BD Pharmingen, #553142) was used to block Fc receptors on cells. Total T cells were stained by Anti-CD3-PE (BD pharmingen, clone 145-2c11, #553064) for 30 minutes on ice. Fixation/Permeabilized (eBioscience) was used to fix and permeabilize cells. Then activated cytotoxic T cells was further stained with Anti-Granzyme B-pacific blue (BioLegend, clone GB11, #515408) and T regulatory cells were stained with Anti-FOX3P-APC (eBioscience, clone FJK16s, #17-

5773-83). The stained cells were washed and analyzed by flow cytometry LSR II (BD Canto II, New Jersey, USA). Details of flow cytometry analysis can be found in our previous report[38].

Western blot

BMDM or RAW 264.7 cells (American Type Culture Collection) were cultured RPMI supplemented with 5% FBS in 37^{o}C incubator with 5%CO_2. 2x10^6 cells were seeded in 12-well plate. After drug treatment, cells were lysed in 0.3ml protein loading buffer (for 20ml buffer, 10% SDS 4ml, Tris-HCL pH6.8 0.75ml, 10% glycerol 5ml, β-mercaptoethanol 0.5ml, and bromophenol blue) for each well, and sonicated for 30s to break DNA. Then cell extracts were electrophoresed through Mini PROTEAN® TGXTM Precast gels (12%, 15well comb, 15ul/well Cat. #456-1046) in a running buffer (10×, Tris 30g, Glycine 144g, SDS 10g, with DD H2O) and transferred to the nitrocellulose membrane (Bio-Rad Laboratories, Inc) in a transfer buffer (Tris 30g, Glysine 144g, SDS 0.5g). The membrane was blocked and probed in TBS-T buffer (TBST +1% Tween, AB14330-01000, American Bioanalytical) containing non-fat milk 1:5000 (Blotting-Grade Blocker, Cat. #170-0604 Nonfat dry milk). Primary antibodies (PD-1 (D7D5W) XP® Rabbit mAb #84651S Mouse Specific lot:1 Ref: 08/2017) at 1:1000 in TBS-T buffer (TBST +1% Tween, AB14330-01000, American Bioanalytical) were incubated with the membrane for shaking overnight at 4°C. Histone, H3 was used as an internal control for normalization and detected with a monoclonal actin antibody diluted at 1:1000 (H3(D1H2) XP® Rabbit mAb #4499S Ref: 06/2017). After washing with TBS-T three times, each time for 5min, the membranes were then further incubated with goat anti-rabbit IgG-HRP SC-2004, lot #B1711 HRP conjugated 1:5000, and incubated in room temperature for 1 hour. Then the membrane was washed with TBS-T three times again. Stable Peroxide Solution 1ml (SuperSignalTM West Pico PLUS, Prod#1863097) and Luminol/Enhancer Solution 1ml (SuperSignalTM West Pico PLUS, Prod#1863096) were used for visualizing, and scan with densitometer. Antibody list: PD-1 (D7D5W) XP® Rabbit mAb #84651S Mouse Specific lot:1 Ref: 08/2017 (Cell signaling), Anti-PD-L1 antibody [EPR20529]ab213480, Arginase-1 (D4E3MTM) XP® Rabbit mAb#93668 (Cell signaling), iNOS Antibody (Mouse Specific) #2982 (Cell signaling), Jak1(6G4)Rabbit mAb#3344 (Cell signaling), P-Jak1 (Y1034/1035)(D7N4Z) Rabbit mAb#74129 (Cell signaling), Jak2(D2E12) XP® Rabbit mAb #3230(Cell signaling), P-Jak2(Y1008)(D4A8) Rabbit mAb #8082 (Cell signaling), Stat1 Antibody#9172(Cell signaling), Phospho-Stat1(Tyr701) (D4A7)Rabbit mAb#7649(Cell signaling), Stat2(D9J7L)Rabbit mAb#72604(Cell signaling), Phospho-Stat2(Tyr690)-R sc-21689 #K1609(SantaCruz), Stat6(D3H4)Rabbit mAb#5397(Cell signaling), Phospho-Stat6(Tyr641)(D8S9Y)Rabbit mAb#56554(Cell signaling), IRF-1(D5E4) XP® Rabbit mAb #8478(Cell signaling), IRF-4(D9P5H)Rabbit mAb#15106(Cell signaling).

Quantitative real time RT-PCR

Total RNA was extracted with TRIzol reagent (Invitrogen, California, USA). The aqueous phase was collected and then one volume of ethanol was added, following the manufacturer's instructions. Before centrifuging, this slurry was added to a column (miRNeasy, Qiagen, Venlo, Limburg) for further extraction and simultaneous DNA digestion (RNase-Free DNAse set, Qiagen). cDNA was synthesized using random primers and reverse transcriptase MMLV (New England Biolabs, Ipswich, MA). qPCR

assays were performed using iTaq™ SYBR® Green Supermix and the CFX96 Real-Time PCR Detection System (Bio-Rad Laboratories, Hercules, CA). Primer sets were listed in the supplementary method. The mouse primer pair sequences are attached in supplementary methods and β-actin serves as internal control (please see supplementary methods for primer sequences). Relative expression of target genes against β-actin was expressed as $2^{-\Delta Ct}$ and fold differences was calculated as expressed mRNA of YIV-906 and or antiPD1-treated samples against untreated samples. Primers sequences are listed (**Table S1**) and the rest of primers that could be found in our previous reports [13,15].

Cytokine analysis by cytometric bead array

Animal plasma and tumor tissue of YIV-906 and or antiPD-1-treated mice and control mice were collected after 96 hours following the treatments. Culture medium of untreated and YIV-906-treated BMDMs were collected after 24 hours exposure. Determination of cytokine expression (IL-6, MIP-1a, IL-5, IL-17A, IL-12p70, TNFa, IL-1B, IL-10, MIG, IFN-r, MCP-1, G-CSF) was performed using cytometric bead array flex set kit by flow cytometry (BD Canto II, New Jersey, USA) according to the manufacturer's instructions (BD biosciences, UK)[15].

Isolation of Bone Marrow Derived Monocytes (BMDMs) and macrophage differentiation

Bone marrow cells were collected from tibias and femurs of 10-week-old C57Bl/6 mice were cultured with complete RPMI-1640 medium (supplemented with 5% Fetal Bovine Serum and 1% Penn/Strep) in the presence of murine M-CSF (10 ng/ml) for 7 days to allow differentiation of monocytes into macrophages[39]. Macrophage were cultured in 5% FBS RPMI-1640 medium with IFNγ (10 ng/ml) to induce polarization to M1-like macrophage while M2-like macrophage were induced by IL4 (20 ng/ml).

IDO Activity Assay

$2x10^6$ HEK293 cells were transfected with mouse IDO (2ug/10cm plate) (OriGene Technologies, Inc., Rockville, MD, Ido1 (NM_008324)) or without IDO DNA as negative control using lipofectamine 3000 for 48h. For one plate, 1ml PBS was used to collect cells into a 2ml tube. Cells were spin down at 3500 rpm 1min. Cells were then sonicated in ice cold 1ml PB buffer pH6.5. Cell lysis was clarified by centrifuging at 12000rpm for 5min at 4^{o}C. 25ul cell lysis will be mixed with 25ul herbal extract at desired concentration and 50ul reaction buffer: (PB buffer 100mM pH 6.5) every 10ml add 70mg Vitamin C, 10ul methylene blue (2.5%), 100ul catalase (20mg/ml), 250ul of 500mM L-tryptophan. Mixture was incubated for 1.5h at 37^{o}C in water bath. Trichloroacetic acid 30% 25ul will be added and incubated at 50^{o}C for 1hr. Finally, Enrlich 0.8% (80mg/10ml in acetic acid) 100ul was added. Absorbance at 540nm will be measure[40]. Optical density at 540nm (Yellow) has positive correlation to the amount of Kynurenine[40].

LC-MS detection

Each tumor sample were homogenized in 200 µL acetronitrile/methanol/water(2/2,1, v/v/v) and 1 mm glass beads (BioSpec Products, Bartlesville, OK) for 30 s at 3500 rpm twice. The homogenate was then

centrifuged at 12000 rpm for 15 min at 4 ^{o}C. The supernatant was dried down in a Speedvac. The residue of each tumor sample was re-dissolved in 100 µL of acetonitrile, and vortexed at 3000 rpm for 3 min. The solution was then centrifuged at 12,000 rpm at 4 ℃ for 15 min, and 2 µL supernatant was injected into the UPLC-QTOF system for analysis. All sample analyses were performed on an ACQUITY ultra-performance liquid chromatography (UPLC) system coupled with a quadrupole-time of flight (Q-TOF) MS instrument (UPLC Xevo G2-XS QTOF MS, Waters Corp., Milford, MA, USA) with an electrospray ionization (ESI) source. Separation was carried out on a Waters ACQUITY BEH C18 column (2.1 X100 mm id, 1.7 µ m) with a guard column (Waters ACQUITY BEH C18 column (2.1 X5 mm id, 1.7 µ m)). The mobile phase consisted of acetonitrile (A) and water containing 0.1% formic acid (B) using a gradient elution of 5% A at 0–2 min, 5–10% A at 2–3 min, 10–17% A at 3–10 min, 17–30% A at 10–15 min, 30–40% A at 15–20 min, 40–80% A at 20–25 min, 80% A at 25–30 min, 80–5% A at 30–31 min, and 5% A at 31–35 min. The flow rate was 0.3 mL/min. Mass spectrometry was performed on a Water Xevo G2-XS QTOF. The scan range was from 50 to 1000 Da. For negative electrospray mode, the capillary voltage and cone voltage were set at 2.5 kV and 60 V, respectively. The desolation gas was set to 800 L/h at a temperature of 500 °C; The cone gas was set to 50 L/h at a temperature of 120 ℃; Data acquisition was achieved using MS^{E}, and the collision energy was 15-60 V.

Statistical Analysis

Data were analyzed by one- or two-way analysis of variance (ANOVA) (GraphPad Prism 7), correlation analysis (GraphPad Prism 7) and Student's t test (Microsoft Office Excel). The difference was statistically significant when $P < 0.05$.

Declarations

Conflict of Interest

Yung-Chi Cheng is the inventor of the use of YIV-906 with Anti-PD1 and Anti-PDL1 for treatment of cancer. The patent is owned by Yale University. Yale University had licensed this patent to Yiviva. S.H Liu, William Cheng and Peikwen Cheng are employed by Yivvia. Wing Lam and Fulan Guan are consultant for Yiviva Inc. The rest of authors had no conflicts interests.

Acknowledgements

This work was supported by the National Cancer Institute(PO1CA154295-01A1), the National Center for Complementary and Alternative Medicine(NCCAM), the Office of Dietary Supplements at the U.S. National Institutes of Health and Yiviva Inc. Yung-Chi Cheng is a fellow of National Foundation for Cancer Research, USA.

Author Contributions

Xiaochen Yang and Wing Lam contributed equally to this work.

Xiaochen Yang did macrophage polarization experiments and wrote the manuscript.

Wing Lam did qRT-PCR, IDO assay, western blot, T cells staining. He designed experiments, interpreted the results, and wrote the manuscript.

Zaoli Jiang did animal experiments.

Xue Han did flow cytometry analysis.

Fulan Guan did immunohistochemistry staining and western blot.

Rong Hu purified Anti-PD1 antibody and IDO assay.

Wei Cai, Yuping Cai, Nicholas J.W. Rattray, Caroline H. Johnson did LC-MS analysis.

William Cheng did macrophage M1/M2 analysis.

Shwu-Huey Liu provided YIV-906 and discussed results.

Peikwen Cheng provided YIV-906 and wrote the manuscript.

Lieping Chen provide anti-PD1 antibody and designed experiment.

Yung-Chi Cheng designed experiment and wrote the manuscript.

References

1. El-Serag, H.B. Hepatocellular carcinoma. *N Engl J Med* **365**, 1118-1127 (2011).
2. Llovet, J.M. & Bruix, J. Molecular targeted therapies in hepatocellular carcinoma. *Hepatology* **48**, 1312-1327 (2008).
3. Wilhelm, S.M.*, et al.* BAY 43-9006 exhibits broad spectrum oral antitumor activity and targets the RAF/MEK/ERK pathway and receptor tyrosine kinases involved in tumor progression and angiogenesis. *Cancer Res* **64**, 7099-7109 (2004).
4. Kudo, M.*, et al.* Lenvatinib versus sorafenib in first-line treatment of patients with unresectable hepatocellular carcinoma: a randomised phase 3 non-inferiority trial. *Lancet* **391**, 1163-1173 (2018).
5. El-Khoueiry, A.B.*, et al.* Nivolumab in patients with advanced hepatocellular carcinoma (CheckMate 040): an open-label, non-comparative, phase 1/2 dose escalation and expansion trial. *Lancet* **389**, 2492-2502 (2017).
6. Tilton, R.*, et al.* A comprehensive platform for quality control of botanical drugs (PhytomicsQC): a case study of Huangqin Tang (HQT) and PHY906. *Chin Med* **5**, 30 (2010).
7. Lam, W.*, et al.* Mechanism Based Quality Control (MBQC) of Herbal Products: A Case Study YIV-906 (PHY906). *Front Pharmacol* **9**, 1324 (2018).

8. Farrell, M.P. & Kummar, S. Phase I/IIA randomized study of PHY906, a novel herbal agent, as a modulator of chemotherapy in patients with advanced colorectal cancer. *Clin Colorectal Cancer* **2**, 253-256 (2003).
9. Saif, M.W.*, et al.* Phase I study of the botanical formulation PHY906 with capecitabine in advanced pancreatic and other gastrointestinal malignancies. *Phytomedicine* **17**, 161-169 (2010).
10. Kummar, S.*, et al.* A phase I study of the chinese herbal medicine PHY906 as a modulator of irinotecan-based chemotherapy in patients with advanced colorectal cancer. *Clin Colorectal Cancer* **10**, 85-96 (2011).
11. Saif, M.W.*, et al.* First-in-human phase II trial of the botanical formulation PHY906 with capecitabine as second-line therapy in patients with advanced pancreatic cancer. *Cancer Chemother Pharmacol* **73**, 373-380 (2014).
12. Liu, S.H. & Cheng, Y.C. Old formula, new Rx: The journey of PHY906 as cancer adjuvant therapy. *Journal of ethnopharmacology* (2012).
13. Lam, W.*, et al.* PHY906(KD018), an adjuvant based on a 1800-year-old Chinese medicine, enhanced the anti-tumor activity of Sorafenib by changing the tumor microenvironment. *Sci Rep* **5**, 9384 (2015).
14. Wang, E.*, et al.* Interaction of a traditional Chinese Medicine (PHY906) and CPT-11 on the inflammatory process in the tumor microenvironment. *BMC Med Genomics* **4**, 38 (2011).
15. Lam, W.*, et al.* The four-herb Chinese medicine PHY906 reduces chemotherapy-induced gastrointestinal toxicity. *Sci Transl Med* **2**, 45ra59 (2010).
16. Rockwell, S.*, et al.* Preclinical studies of the Chinese Herbal Medicine formulation PHY906 (KD018) as a potential adjunct to radiation therapy. *Int J Radiat Biol* **89**, 16-25 (2013).
17. Lam, W.*, et al.* The number of intestinal bacteria is not critical for the enhancement of antitumor activity and reduction of intestinal toxicity of irinotecan by the Chinese herbal medicine PHY906 (KD018). *BMC Complement Altern Med* **14**, 490 (2014).
18. Intlekofer, A.M. & Thompson, C.B. At the bench: preclinical rationale for CTLA-4 and PD-1 blockade as cancer immunotherapy. *J Leukoc Biol* **94**, 25-39 (2013).
19. Munn, D.H. & Mellor, A.L. Indoleamine 2,3-dioxygenase and tumor-induced tolerance. *J Clin Invest* **117**, 1147-1154 (2007).
20. Holmgaard, R.B.*, et al.* Tumor-Expressed IDO Recruits and Activates MDSCs in a Treg-Dependent Manner. *Cell Rep* **13**, 412-424 (2015).
21. Holmgaard, R.B., Zamarin, D., Munn, D.H., Wolchok, J.D. & Allison, J.P. Indoleamine 2,3-dioxygenase is a critical resistance mechanism in antitumor T cell immunotherapy targeting CTLA-4. *J Exp Med* **210**, 1389-1402 (2013).
22. Zhang, W.*, et al.* Identification of chemicals and their metabolites from PHY906, a Chinese medicine formulation, in the plasma of a patient treated with irinotecan and PHY906 using liquid chromatography/tandem mass spectrometry (LC/MS/MS). *J Chromatogr A* **1217**, 5785-5793 (2010).

23. Ye, M.*, et al.* Liquid chromatography/mass spectrometry analysis of PHY906, a Chinese medicine formulation for cancer therapy. *Rapid Commun Mass Spectrom* **21**, 3593-3607 (2007).
24. Chen, S., Corteling, R., Stevanato, L. & Sinden, J. Natural inhibitors of indoleamine 3,5-dioxygenase induced by interferon-gamma in human neural stem cells. *Biochemical and biophysical research communications* **429**, 117-123 (2012).
25. Spranger, S.*, et al.* Mechanism of tumor rejection with doublets of CTLA-4, PD-1/PD-L1, or IDO blockade involves restored IL-2 production and proliferation of CD8(+) T cells directly within the tumor microenvironment. *J Immunother Cancer* **2**, 3 (2014).
26. Long, G.V.*, et al.* Epacadostat plus pembrolizumab versus placebo plus pembrolizumab in patients with unresectable or metastatic melanoma (ECHO-301/KEYNOTE-252): a phase 3, randomised, double-blind study. *Lancet Oncol* **20**, 1083-1097 (2019).
27. Le Naour, J., Galluzzi, L., Zitvogel, L., Kroemer, G. & Vacchelli, E. Trial watch: IDO inhibitors in cancer therapy. *Oncoimmunology* **9**, 1777625 (2020).
28. Genard, G., Lucas, S. & Michiels, C. Reprogramming of Tumor-Associated Macrophages with Anticancer Therapies: Radiotherapy versus Chemo- and Immunotherapies. *Front Immunol* **8**, 828 (2017).
29. De Palma, M. & Lewis, C.E. Macrophage regulation of tumor responses to anticancer therapies. *Cancer Cell* **23**, 277-286 (2013).
30. Hoves, S.*, et al.* Rapid activation of tumor-associated macrophages boosts preexisting tumor immunity. *J Exp Med* **215**, 859-876 (2018).
31. Gordon, S.R.*, et al.* PD-1 expression by tumour-associated macrophages inhibits phagocytosis and tumour immunity. *Nature* **545**, 495-499 (2017).
32. Chen, W., Wang, J., Jia, L., Liu, J. & Tian, Y. Attenuation of the programmed cell death-1 pathway increases the M1 polarization of macrophages induced by zymosan. *Cell Death Dis* **7**, e2115 (2016).
33. Dhupkar, P., Gordon, N., Stewart, J. & Kleinerman, E.S. Anti-PD-1 therapy redirects macrophages from an M2 to an M1 phenotype inducing regression of OS lung metastases. *Cancer Med* **7**, 2654-2664 (2018).
34. Cheng, L., Wang, Y. & Huang, L. Exosomes from M1-Polarized Macrophages Potentiate the Cancer Vaccine by Creating a Pro-inflammatory Microenvironment in the Lymph Node. *Mol Ther* **25**, 1665-1675 (2017).
35. Pozzi, L.A., Maciaszek, J.W. & Rock, K.L. Both dendritic cells and macrophages can stimulate naive CD8 T cells in vivo to proliferate, develop effector function, and differentiate into memory cells. *J Immunol* **175**, 2071-2081 (2005).
36. Liu, S.H. & Cheng, Y.C. Old formula, new Rx: the journey of PHY906 as cancer adjuvant therapy. *J Ethnopharmacol* **140**, 614-623 (2012).
37. Tan, H.Y.*, et al.* Autophagy-induced RelB/p52 activation mediates tumour-associated macrophage repolarisation and suppression of hepatocellular carcinoma by natural compound baicalin. *Cell Death Dis* **6**, e1942 (2015).

38. Han, X., *et al.* The development and functions of CD4(+) T cells expressing a transgenic TCR specific for an MHC-I-restricted tumor antigenic epitope. *Cell Mol Immunol* **8**, 333-340 (2011).
39. Weischenfeldt, J. & Porse, B. Bone Marrow-Derived Macrophages (BMM): Isolation and Applications. *CSH Protoc* **2008**, pdb prot5080 (2008).
40. Braun, D., Longman, R.S. & Albert, M.L. A two-step induction of indoleamine 2,3 dioxygenase (IDO) activity during dendritic-cell maturation. *Blood* **106**, 2375-2381 (2005).

Figures

Figure 1

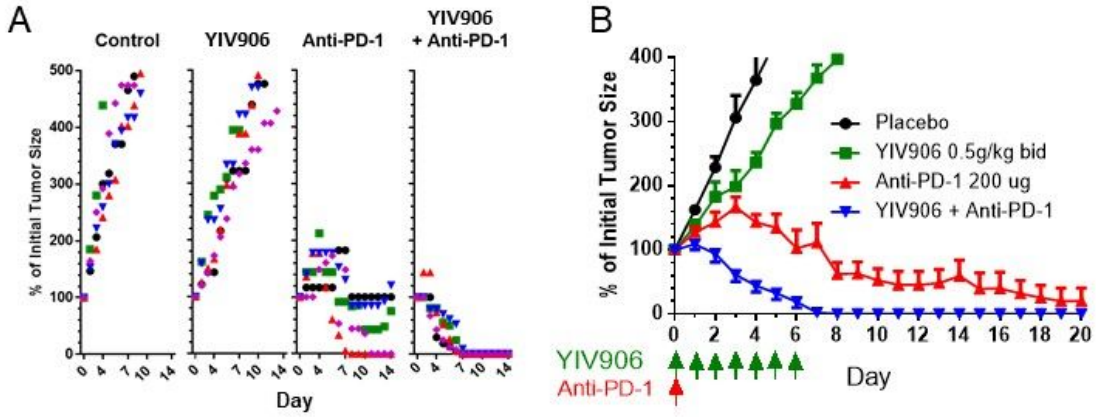

Figure 1

Effect of YIV-906 on the anti-tumor of Anti-PD1 (YIV-906 500mg/kg p.o. bid x7, Anti-PD-1 antibody 200ug/mice i.p. once) against Hepa 1-6 tumor growth of C57BL6 mice. (A) Individual tumor growth (indicated as spot plot with different colors and symbols) of each treatment group during day 0 to 14. (B)

Average(±SD) tumor growth of each treatment group during day 0 to 20. Tumor size at the beginning were about 180mm3. Details of experimental procedures are given in Materials and Methods.

Figure 2

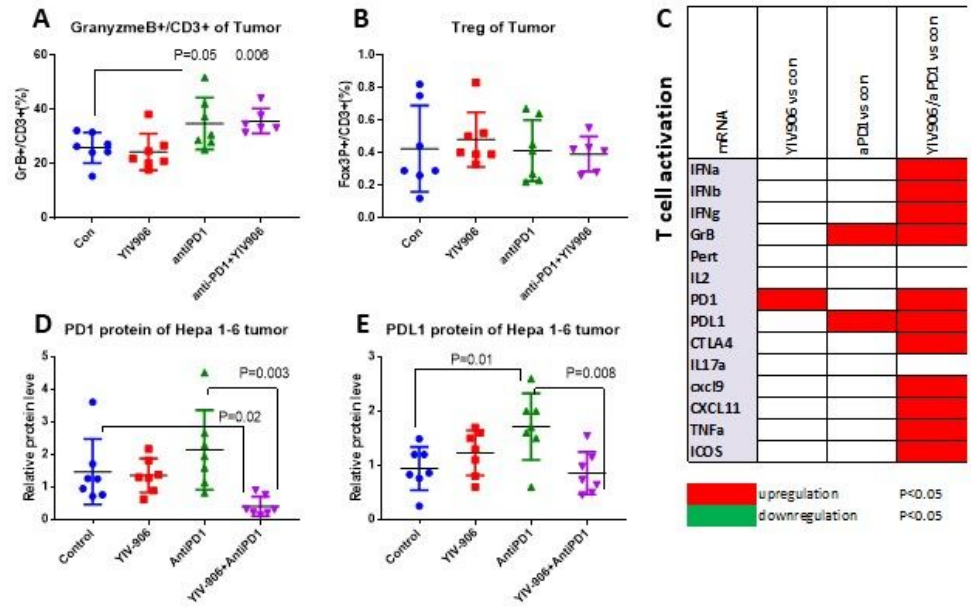

Figure 2

Figure 2.Effect of YIV-906 and/or Anti-PD1 on PD1/PDL1 protein expression and T cell activity. (A) Effect of YIV-906 and/or Anti-PD1 on activated T cell of Hepa 1-6 tumor as indicated by GranyzmeB and CD3 staining. (B) Effect of YIV-906 and/or Anti-PD1 on Treg cell of Hepa 1-6 tumor as indicated by CD3+/FOX3P+. Following 4 day treatment, tumor tissues were digested by dispase and subsequently stained with fluorescence labelled antiFOX3P or antiGranyzme B together with CD3(T cells) and CD45(blood cells). Flow cytometer analysis was used to determined the percentage of Treg or GranyzmeB+ve cells of total T cells. (C) Effect of YIV-906 and/or Anti-PD1 on mRNA expression related to T cell of Hepa 1-6 tumor. Using qRT-PCR. T-test P values were shown in the graph. The PD1 (D) and PDL1 (E) protein expression of Hepa 1-6 tumor following YIV-906 and/or Anti-PD1 treatment. Western blot analysis for the PD1 and PDL1 protein expression of Hepa 1-6 tumor following 4 days treatment of Anti-PD1-/+YIV-906. Beta-actin was used for normalization of protein loading. Each sample was normalized

to a master mix sample (MIX) which loading duplicated in each gel. Details of experimental procedures are given in Materials and Methods.

Figure 3

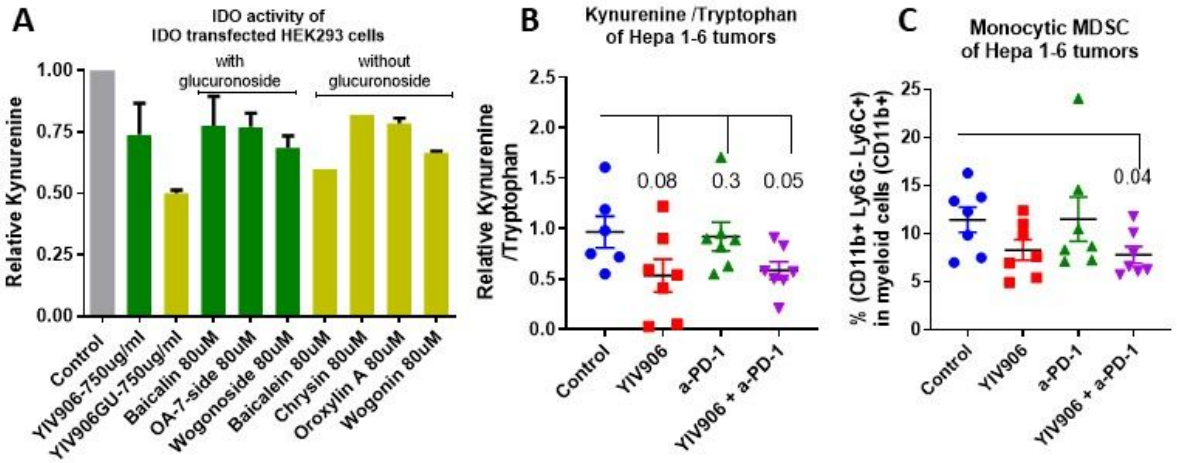

Figure 3

Effect of YIV-906 on IDO activity in vitro and in vivo. (A) Effect of YIV-906, E.coli glucuronidase treated YIV906 (YIV906GU), and its flavonoids on IDO activity of IDO transfected HEK293 cells in culture. HEK293 cells were transfected with mouse IDO expression plasmids and then seeded for culturing overnight. L-tryptophan 125uM with or without YIV906, YIV906GU or its flavonoids were added to the wells for 24hr. The concentration of kynurenine of culture medium was measured using colorimetric based assay. Results were normalized to protein concentration in each well. (B) Effect of different treatments on Kynurenine/tryptophan of Hepa 1-6 tumors. (C) Effect of different treatment on monocytic MDSC of Hepa 1-6 tumors. P values from T-test are indicated in the B, C.

Figure 4.

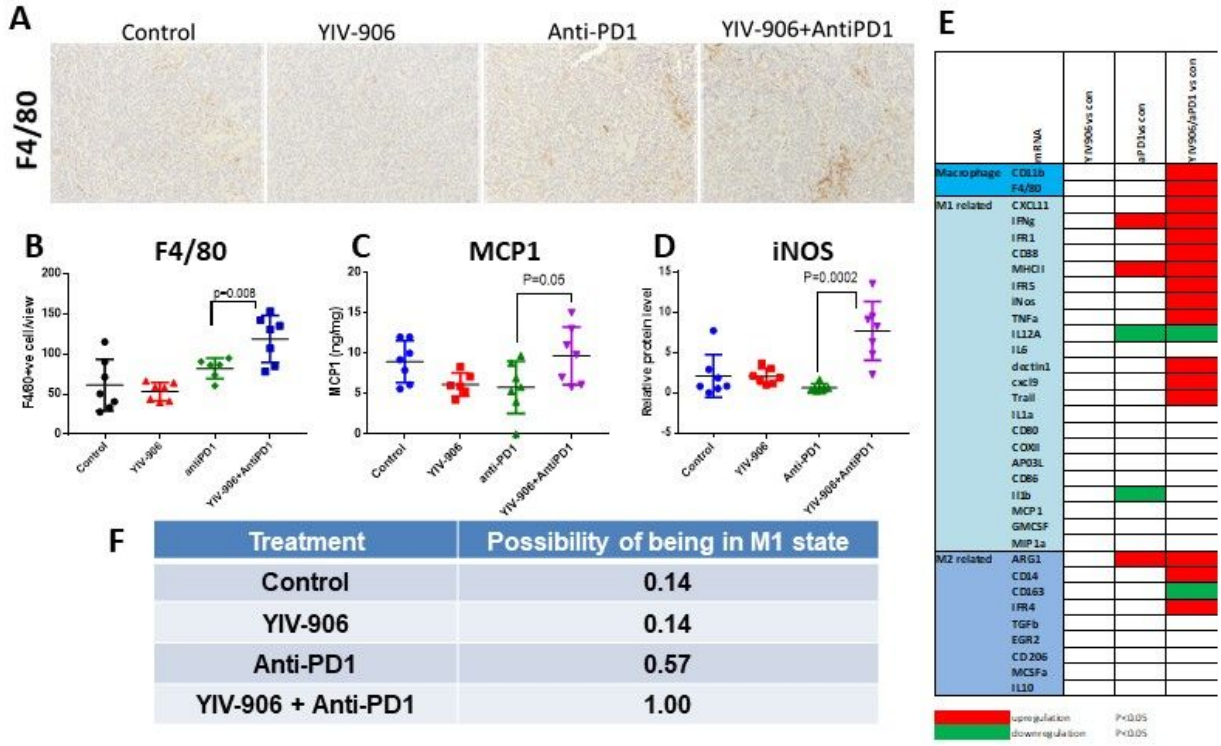

Treatment	Possibility of being in M1 state
Control	0.14
YIV-906	0.14
Anti-PD1	0.57
YIV-906 + Anti-PD1	1.00

Figure 4

Impact of YIV906 and/or aPD1 on macrophages and M1/M2 signature genes expression of Hepa 1-6 tumor. (A) Immunohistochemistry staining of F4/80 for macrophage infiltration into Hepa 1-6 tumor after 4-day treatments. (B) Quantification of macrophage of tumor sections after 4-day treatments. (C, D) MCP1 and iNOS protein expression of Hepa 1-6 tumor after 4-day treatments. (E) Heat map (significantly be up-regulated: red, significantly by down regulated: green) for indicating the mRNA expression determined by RT-qPCR following treatment at day 4. (F) Possibility of being M1 state based on the signature gene expression of (A). P values were obtained from T-test analysis. Details of experimental procedures are given in Materials and Methods.

Figure 5.

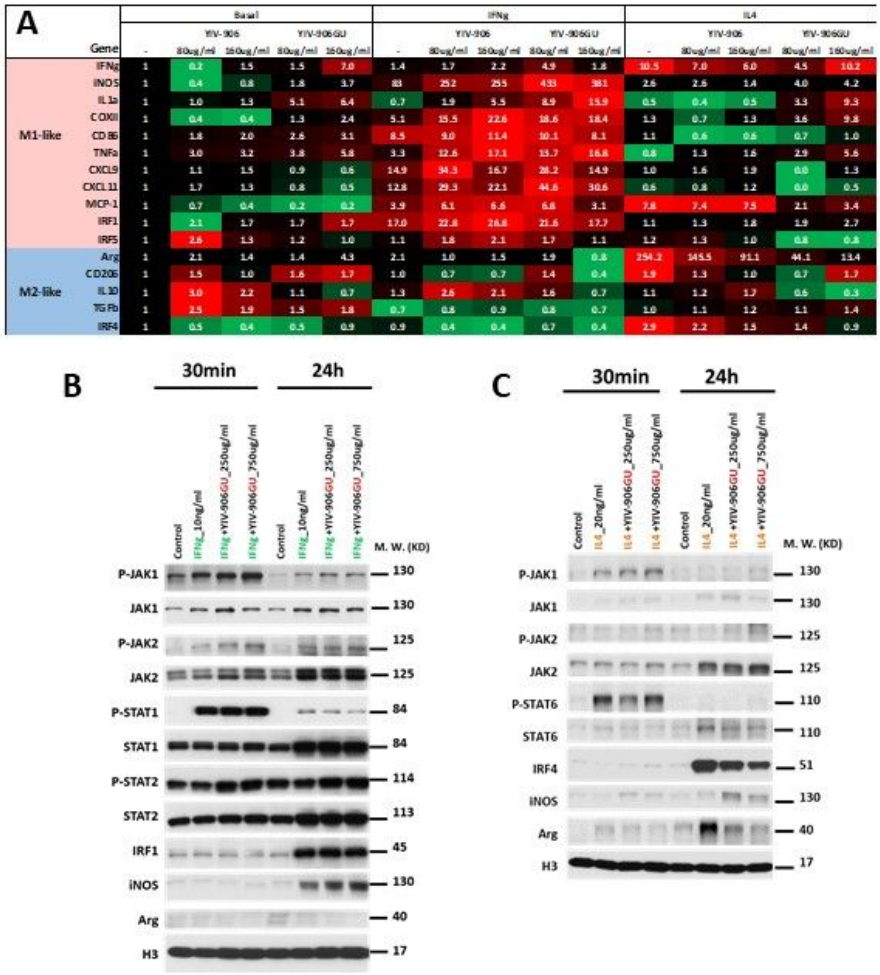

Figure 5

Effect of YIV-906 on the action of INFg or IL4 on polarizing bone marrow derived macrophage (BMDMs) into M1 or M2-like macrophage. (A) Heat map for the mRNA expression levels of BMDM following INFg or IL14 with or without YIV-906/GU treatment. For each row (gene), up-regulation of mRNA is highlighted as (red) while down-regulation is highlighted as (green). Number of the table shows the relative fold change gene expression in each treatment conditions (average of three independent experiment and all gene expressions were normalized to actin). (B) Western blot analysis for the effect of YIV-906GU on the action of IFNg on IFNg signaling of BMDMs. Cropped blots are used in this figure and they have been run under the same experimental conditions. (C) Western blot analysis for the effect of YIV-906GU on the action of IL4 on IL4 signaling of BMDMs. Bone marrow cells were cultured in the presence of murine M-CSF (10ng/ml) for 7 days, and then cultured in presence with IFNg 10ng/ml to induce polarization to M1-like macrophage while M2 like macrophage were induced by IL-4 20ng/ml for 24h. YIV-906 or YIV-906GU was added at the same time with IFNg or IL4. The mRNA expression of M1 or M2 related genes were determined by RT-qPCR following treatment at day 8. Protein expression or phosphorylation were detected with western blotting. Histone H3 was used for normalization of protein loading. Cropped blots

are used in this figure and they have been run under the same experimental conditions. Details of experimental procedures are given in Materials and Methods.

Figure 6

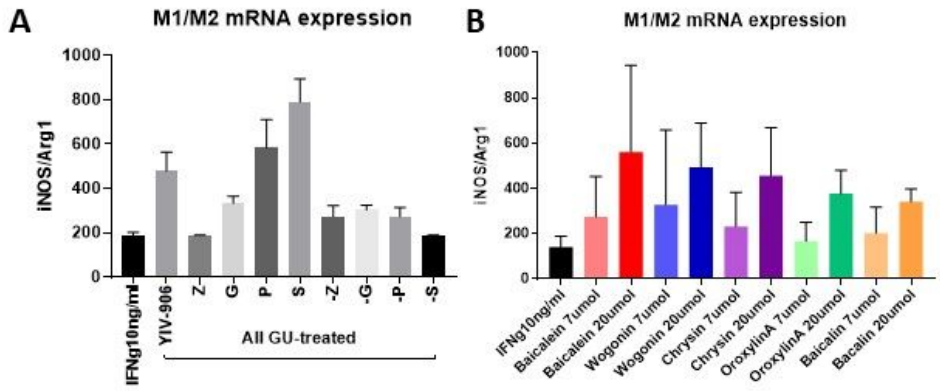

C

Compound	Formula	m/z [M-H]⁻	Hepa 1-6 Tumor	
			YIV-906	YIV-906+Anti-PD1
Baicalein	$C_{15}H_{10}O_5$	269.0458	+	+
Wogonin	$C_{16}H_{12}O_5$	283.0615	+	++
Chrysin	$C_{15}H_{10}O_4$	253.0549	-	-
Oroxylin A	$C_{16}H_{12}O_5$	283.0601	+	++
Baicalin	$C_{21}H_{18}O_{11}$	445.0756	-	-

-: undetected, +: detected, ++: detected with higher amount than +.

Figure 6

Effect of flavonoids of YIV-906 in Potentiating IFNg action. (A) Effect of YIV906GU, single herbs (G, P, S and Z: GU treated) or one herb deleted formulation (-G, -P, -S and –Z: GU treated) on the mRNA expression of iNOS/Arg of macrophage. (B) Effect of baicalein, wogonin, chrysin, oroxylin A and baicalin on the mRNA expression of iNOS/Arg of macrophage. Raw cells were cultured in the presence of murine M-CSF (10ng/ml) for 3 days, and then cultured in presence with IFNg 10ng/ml alone or with YIV-906GU/its components to induce polarization to M1-like macrophage for 24h. The mRNA expression was determined by RT-qPCR following treatment at day 8. (C) Detection of YIV-906 compounds of Hepa 1-6 tumor following oral administration of YIV-906 with or without Anti-PD1 using LC-MS. Details of experimental procedures are given in Materials and Methods.

Supplementary Files

This is a list of supplementary files associated with this preprint. Click to download.

- SupplementalFigures.pptx
- Supplementarytable.docx